

HypBO: Expert-Guided Chemist-in-the-Loop Bayesian Search for New Materials

Abdoulatif Cissé^{1,3}, Xenophon Evangelopoulos^{1,3}, Sam Carruthers^{1,3}, Vladimir V. Gusev², Andrew I. Cooper^{1,3}

¹Department of Chemistry, University of Liverpool, England, UK

²Department of Computer Science, University of Liverpool, England, UK

³Leverhulme Research Centre for Functional Materials Design, University of Liverpool, England, UK
{abdoulatif.cisse, evangx, sgscarru, vladimir.gusev, aicooper}@liverpool.ac.uk

Abstract

Robotics and automation offer massive accelerations for solving intractable, multivariate scientific problems such as materials discovery, but the available search spaces can be dauntingly large. Bayesian optimization (BO) has emerged as a popular sample-efficient optimization engine, thriving in tasks where no analytic form of the target function/property is known. Here we exploit expert human knowledge in the form of hypotheses to direct Bayesian searches more quickly to promising regions of chemical space. Previous methods have used underlying distributions derived from existing experimental measurements, which is unfeasible for new, unexplored scientific tasks. Also, such distributions cannot capture intricate hypotheses. Our proposed method, which we call HypBO, uses expert human hypotheses to generate an improved seed of samples. Unpromising seeds are automatically discounted, while promising seeds are used to augment the surrogate model data, thus achieving better-informed sampling. This process continues in a global versus local search fashion, organized in a bilevel optimisation framework. We validate the performance of our method on a range of synthetic functions and demonstrate its practical utility on a real chemical design task where the use of expert hypotheses accelerates the search performance significantly.

1 Introduction

Bayesian Optimization (BO) has emerged as a valuable tool for optimizing experiments in fields such as chemistry and materials science, where experiments are costly and time-consuming (Shahriari et al. 2016). Traditional experimental design methods often involve exhaustive exploration of the parameter space. By contrast, BO offers an efficient framework that leverages Bayesian inference to guide the iterative exploration of the space, ultimately maximizing the target experiment property (Jones, Schonlau, and Welch 1998).

Formally, BO aims to find the global optimum in the following problem:

$$x^* = \underset{x \in \mathcal{X}}{\operatorname{argmax}} f(x), \quad (1)$$

where $f : \mathcal{X} \rightarrow \mathbb{R}$ is a continuous function over the d -dimensional input space $\mathcal{X} \in \mathbb{R}^d$. Generally, the underlying

analytical form of $f(\cdot)$ is unknown. This makes it a black-box function, as the experimenters only have access to the input-output behavior of the function without any knowledge of its internal workings. The core principle of BO lies in the construction of a probabilistic model, typically a Gaussian Process (GP) (Ebden 2015), which serves as a *surrogate model* for $f(\cdot)$. This surrogate model is updated iteratively as new experimental data become available, allowing for the refinement of target predictions. The model’s uncertainty is quantified and an *acquisition function* is employed to select the next set of experimental parameters to evaluate, balancing exploration (sampling in unexplored regions) and exploitation (focusing on promising regions).

Injecting domain-specific knowledge into BO to accelerate and boost optimization performance has gained significant recent attention, especially for scientific tasks (Ramachandran et al. 2020), aiming to alleviate the resource-intensive surrogate model construction. In particular, recent studies have used expert knowledge in the form of user-specified priors over possible optima to guide the search toward promising regions (Hvarfner et al. 2022; Li et al. 2020). While this has shown promising performance in a variety of tasks, it is difficult in many scientific problems to realize external knowledge in a form of a prior distribution. Furthermore, the optimization landscapes of such problems often resemble a needle-in-a-haystack manifold (Siemenn et al. 2023) and the use of inaccurate prior knowledge distributions can hinder the induction of negative bias in the problem and quickly degrade performance. More recently, human-in-the-loop (HIL) approaches have emerged where an interactive optimization framework enables experts to implicitly add knowledge to the problem in a form of feedback on the quality of the samples within the experimental loop (Huang et al. 2022). However, this type of knowledge is implicit and sample-specific, and can in practice lead to local optima entrapment. Another category of methods introduce domain-specific knowledge in the form of hard constraints in the problem (Hernández-Lobato et al. 2015), which can however over-restrict the search in practice.

In this paper, we propose a novel approach to inject domain knowledge using input from domain experts to direct the search to more fruitful regions. We specifically represent domain knowledge as human hypotheses or conjectures that are realized as intervals of confidence within the search

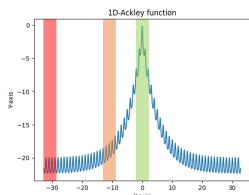


Figure 1: Illustration of three hypothesis locations in the form of confidence regions on the 1D Ackley function. The different colors (red, orange, green) correspond to different levels of confidence (poor, weak, and good, respectively).

space. Figure 1 demonstrates three representative hypothesis regions within the input space of a one-dimensional Ackley function where the input region around zero is clearly the most promising hypothesis. We model the various hypotheses as local Gaussian processes (GPs) to distil their utility, which is in turn evaluated by a global GP, and the search space is expanded accordingly. Our approach comes with the major benefit of provably neither over-restricting the search, nor getting stuck in local hypothesis optima, but rather treating hypotheses as a warm-start for the optimization towards a more adventurous search. We formulate our approach in a bilevel optimization framework where the lower level evaluates the various hypotheses and the upper level integrates the useful ones in the search.

We test the proposed methodology on a materials design simulation where a set of different chemical hypotheses are injected to warm-start the problem. We show that hypotheses with favorable conditions accelerate the search and also improve performance. Interestingly, unfavorable hypotheses do not appear to negatively bias the search in the long run. Extensive synthetic tests further demonstrate that our method maintains a competitive and robust performance overall.

The remainder of this paper is organized as follows. Section 2 presents recent works about expert knowledge integration in BO, while Section 3 describes the proposed methodology. The robustness and performance of our algorithm are evaluated and discussed in Section 4. Finally, Section 5 summarizes our work and introduces future directions.

2 Related Works

Some research teams have used transfer learning recently (Niu et al. 2020) to extract and use knowledge from previous BO executions to aid in warming up and enhancing optimization (Theckel Joy et al. 2019). This can address the BO ‘cold start’ problem, where the initial points, usually selected randomly, fail to capture adequately the optimization objective’s landscape. Transfer learning has also been used effectively in chemical reaction optimization (Hickman et al. 2023) to bias the search space by weighting the current acquisition function with past predictions. However, it does not fold in expert domain knowledge or hypotheses.

Other approaches inject expert prior beliefs from a fixed set of distributions to guide the optimization process. Li et al. 2020 combined prior user beliefs with observed data to compute the posterior distribution via repeated Thompson

sampling. This approximates new sampling points using a linear combination of posterior samplings. BOPrO (Souza et al. 2021) uses a prior that is provided by the user and a data-driven model to generate a pseudo-posterior. Similarly, π BO (Hvarfner et al. 2022) generates a pseudo-posterior by integrating prior beliefs into the acquisition function as a decaying multiplicative factor to improve sampling. Both of these methods are limited to one expert prior, and the use of priors cannot capture intricate knowledge. Ramachandran et al. 2020 employ the probability integral transform to manipulate the search space by stretching regions with high probability and compressing others. However, this approach requires invertible priors and lacks empirical evidence of its ability to recover from poor priors.

Another promising approach to improving BO involves the use of similarities between points in the search space to incorporate domain knowledge. Gryffin (Häse et al. 2021), for example, uses user-provided physicochemical descriptors to navigate the search space more efficiently by identifying similarities between individual options based on those descriptors. However, when using a large number of descriptors (e.g., hundreds), spurious correlations can occur between descriptors and the optimized objective, leading to some irrelevant descriptors being considered important. Morishita and Kaneko 2023 suggest using a clustering-based initial sample selection method for optimizing chemical reaction conditions with BO, based on high correlation between molecular descriptors and clustering in chemical space. However, as clustering is based on unsupervised learning, there is a need for expert knowledge to connect it with experimental results; also, not all scientific problems can be codified using molecular descriptors.

Preference learning can also add knowledge to BO. Huang et al. 2022 obtain expert opinions by querying them with pairwise comparisons, thereby approximating the shape of the objective function. A V et al. 2022 take a slightly different approach by allowing experts to provide a pair of good and bad points, which are then used to fine-tune the BO’s surrogate model by replacing its current optimal hyperparameters with ones that align more closely with the expert’s cognitive model. Such approaches are promising but risk biasing the optimizer, which could ultimately mimic the user’s beliefs and result in suboptimal solutions.

Various methods can restrict the search space to regions believed by the optimizer to contain the optimum. TurboBO (Eriksson et al. 2019) uses multiple independent GP surrogate models within different trust regions to conduct simultaneous BO runs, and a multi-armed bandit (MAB) strategy to choose which local optimizations to continue. TREGO (Diouane et al. 2021) proposed alternating between global BO and a trust region-based policy for the local phase when the global BO is failing. Alternatively, LA-MCTS (Wang, Fonseca, and Tian 2020) proposes the use of Monte Carlo tree search to learn which subregions of the search space are more likely to contain good objective values. The space is then recursively partitioned based on optimization performance. Similarly, ZoMBI (Siemenn et al. 2023) iteratively keeps the best sample points found so far and zooms in the sampling search bounds towards the region formed by those

samples. However, none of these approaches uses intricate expert knowledge in the form of multiple hypotheses to further improve the search. Here, we propose a generalized strategy to inject multiple expert hypotheses, such as derived from a multi-person research team, where promising seeds from those hypotheses augment BO’s surrogate model data to achieve better-informed sampling.

3 Methodology

In this section, we propose a novel BO methodology that uses experts’ background knowledge in a form of optimality hypotheses to guide search space exploration more effectively. Let $\{\mathcal{H}_j\}_{j=1}^J$ be a set of hypotheses w.r.t. promising areas (subspaces) formulated in hyperrectangles and specified by a system of p equations and q inequalities describing an interval of confidence in the search space

$$\begin{aligned} Ax &= b, \\ Bx &\leq c, \end{aligned} \quad (2)$$

where $A \in \mathbb{R}^{p \times d}$ and $B \in \mathbb{R}^{q \times d}$ are coefficient matrices, and $b \in \mathbb{R}^p$ and $c \in \mathbb{R}^q$ are solution vectors. This system filters the space \mathcal{X} and forms a solution set, which we refer to as hypothesis subspace \mathcal{H}_j .

Our goal is to inject practitioners’ expertise into the problem at hand by attending to specific regions of the search space based on domain hypotheses, minding at the same time not to over-restrict and negatively bias the search. We therefore formulate the various different hypotheses as *local* GPs using their output samples as *seeds* for the *global* search. The utility of the seeds can be measured using any standard acquisition function, and the top-performing seeds are selected and fed through to the global search. This iterative global-versus-local search is realized interchangeably, thus helping to avoid negatively biasing the search and getting stuck in local optima. We specifically formulate this Bayesian search in a parametric bilevel optimization framework, which in this instance can be solved sequentially as a two-stage decision problem with each level’s variables treated as a parameter for the other (Köppe, Queyranne, and Ryan 2010). The following paragraphs detail and formalize the proposed optimization framework.

Upper level In this level we seek to find the global maximum of $f(\cdot)$ in (1) as in any standard BO task where an acquisition function $\alpha(\cdot)$ is maximized to obtain new candidate samples and evaluate them across its iterations

$$x^* = \underset{x \in \mathcal{X}}{\operatorname{argmax}} \alpha(x, \mathcal{D}) \quad (3)$$

with $\mathcal{D} = \{x_i, y_i = f(x_i)\}_{i=1}^n$ being the observation dataset. To compute $\alpha(\cdot)$, BO relies on constructing a global surrogate model of the underlying function and greatly depends on the initial samples provided as a seed when building this. An appropriate initial sample selection has shown to significantly improve the performance of the search in practice (Morishita and Kaneko 2023). At this level, one could use practically any variant of BO, but we have empirically observed that using the LA-MCTS algorithm (Wang, Fonseca, and Tian 2020) helps the search to focus on promising regions to avoid over-exploring.

Lower level The lower level initially uses the subspaces from the given hypotheses to perform a *local* search and yield a set of best-performing seed samples $\{s_t\}_{t=1}^T$, with $T < J$, essentially acting as soft constraints on the target objective function $f(\cdot)$. Given that we do not have any analytical information about $f(\cdot)$, we approximate it in the hypothesis subspaces by multiple local GP models $\phi_j \sim \mathcal{N}(\mu_j(x), k_j(x, x'))$ simultaneously, one for each hypothesis subspace \mathcal{H}_j . The local models ϕ_j are chosen as GP surrogate models for their robustness to noise and uncertainty (Ebden 2015). The local search is realized in a Multi-Armed Bandit (MAB) (Vermorel and Mohri 2005) fashion where getting a seed s_t translates into allocating samples via an implicit policy where the hypotheses are the arms. This allows us to evaluate the various different hypotheses and steer the sampling toward promising regions.

As the optimization progresses, the hypothesis subspaces \mathcal{H}_j will potentially have more samples, which will update the local models, better evaluating the hypotheses and producing better seeds. Stopping criteria for each level and global convergence are discussed below in Section 3.1.

The complete bilevel framework is formalized as follows

$$x^* = \underset{x \in \mathcal{X}}{\operatorname{argmax}} \alpha(x, \{(s_t, f(s_t))\}_{t=1}^T \cup \mathcal{D}) \quad (\text{Upper})$$

s.t

$$\{s\}_{t=1}^T \in \underset{x \in \bigcup_{j=1}^J \mathcal{H}_j}{\operatorname{argmax}} \{ \max_{x \in \mathcal{H}_j} \phi_j \}. \quad (\text{Lower})$$

3.1 Convergence criteria

To maximize the information gain from good hypotheses (true), we allow the lower level to produce more seed samples until it plateaus. That is, the lower level returns seed samples until these fail to improve upon the best target value:

$$f(x^*) < f(s_i) + \gamma \text{ for } i = 1, \dots, m_l, \quad (4)$$

where i is the iteration number, $\gamma \in \mathbb{R}^+$ is the growth step size and $m_l \in \mathbb{N}^+$ dictates after how many consecutive seed samples we deem the lower level plateauing.

To mitigate weak and poor hypotheses (false), we allow the upper level to carry the optimization from the given seeds until it is plateauing. It keeps maximizing α until it fails to improve upon the best target value, that is:

$$f(x^*) < f(x_i) + \gamma \text{ for } i = 1, \dots, m_u, \quad (5)$$

where $m_u \in \mathbb{N}^+$ dictates after how many consecutive samples we deem the upper level failed. We set $m_l \ll m_u$ to direct the search toward the hypotheses’ subspaces if they are helping to improve while still giving the upper level the time to explore the entire search space \mathcal{X} .

The complete steps of the optimization are detailed in Algorithm 1.

4 Experiments

We showcase the effectiveness of our proposed method in optimizing various synthetic functions and real-world problems, such as discovering new materials. We test HypBO’s performance and robustness using hypotheses of different

Algorithm 1: Hypothesis Bayesian Optimization (HypBO)

Input: Upper-level acquisition function α , lower-level acquisitions $\{\alpha_{\phi_j}\}_{j=1}^J$, total number of hypotheses J , maximum iteration number i_{max} , growth step size γ , lower-level failure limit m_l , upper-level failure limit m_u , upper limit of locally optimal samples T .

Output: y_{max}

```
1: Initialize the observation dataset  $\mathcal{D} \leftarrow \{(x_{init}, y_{init})\}$ ;  
2: while  $i < i_{max}$  do  
3:   while not  $(f(x^*) \geq f(s_i) + \gamma, i = 0, \dots, m_l)$  do  
4:     for each hypothesis  $\mathcal{H}_j$  do  
5:       Fit the GP  $\phi_j \sim \mathcal{N}(0, k)$  with  $\mathcal{D} \cap \mathcal{H}_j$ ;  
6:        $s_j = \operatorname{argmax}_x \alpha_{\phi_j}(x)$ ;  
7:     end for  
8:     Keep best performing samples  $\{s_t\}_{t=1}^T$  w.r.t.  $\alpha_{\phi_j}$ ;  
9:   end while  
10:  while not  $(f(x^*) \geq f(x_i) + \gamma, i = 0, \dots, m_u)$  do  
11:    Fit the GP  $\sim \mathcal{N}(0, k)$  with  $\mathcal{D} \cup \{(s_t, f(s_t))\}_{t=1}^T$ ;  
12:     $x^* = \operatorname{argmax}_{x \in \mathcal{X}} \alpha(x, \mathcal{D} \cup \{(s_t, f(s_t))\}_{t=1}^T)$ ;  
13:    Evaluate  $x^*, y^* = f(x^*)$  and  $\mathcal{D} \leftarrow \mathcal{D} \cup \{(x^*, y^*)\}$ ;  
14:  end while  
15:   $i \leftarrow i + 1$ ;  
16: end while  
17: return  $y_{max}$ 
```

qualities, ranging from good to intentionally poor. We also compare its performance against other BO algorithms. In Section 4.1, we outline the various experimental settings and comparison methods that we used to benchmark our results. Sections 4.2 and 4.3 present the outcomes of an analytical function optimization task and a materials design problem (Burger et al. 2020), respectively.

4.1 Experimental Setup

We evaluate HypBO’s performance empirically for the following two tasks:

- **Synthetic Functions** We test the precision, convergence speed, and robustness of HypBO using synthetic benchmark functions with various nonconvex landscapes and dimensionalities. The optimization performance is measured using simple regret. The maximum number of iterations is limited to 100, and the result of 50 repeated trials is reported as the mean value.
- **Photocatalytic Hydrogen Production** Here, we replicate the materials design problem addressed in (Burger et al. 2020), aiming to maximize the hydrogen evolution rate (HER) from a mixture of different materials. We follow a more cost-effective approach and emulate that chemistry experiment by interpolating new HER measurements using a Gaussian process regression (GPR) model trained on existing experimental datapoints. In section 4.3, we give a comprehensive explanation of this chemistry task. The maximum number of iterations is set to 300, and the mean value of 50 repeated trials is reported.

We further evaluate HypBO against the following baselines:

- **Random search (RS)** Random search under uniform distribution over the search space.
- **Latent Action Monte Carlo Tree Search (LA-MCTS)** As described in Section 2, there is no truly direct comparison that can be made with other BO methods as they cannot capture more intricate knowledge in the form of a hypothesis and deal with a range of simultaneous hypotheses. While LA-MCTS cannot use external expert knowledge, its automated partitioning of the search space into subspaces of different confidences emulates the use of hypotheses to direct the search to promising regions. Hence, it a good baseline for HypBO, which gets its partitioning from experts. We set LA-MCTS hyperparameters as follows: C_p to 10, the splitting threshold θ to 10, the kernel to RBF, gamma to auto and the solver to BO.

For all experiments, we use preset hyperparameters for HypBO. We set the growth rate γ to 0, the lower level limit m_l to 2 and the upper level limit m_u to 5. The local GP models for the hypotheses have a zero mean and a Matérn ($\nu = 2.5, \lambda_i = 1$) kernel with constant scaling. All experiments are warm-started with five initial points except for the photocatalyst hydrogen production experiment with mixed hypotheses, whose initial sample count is 10. The benchmark results and code can be found at <https://anonymous.4open.science/r/HypBO/>.

4.2 Synthetic Functions

Hypotheses A good hypothesis subspace is essentially an interval that contains the optimum, opt . By contrast, a weak/poor one does not. The further the weak hypothesis subspace is from the optimum, the worse it is. Here, the “poor” hypothesis is the furthest possible from the optimum. The hypotheses are hyperrectangles of width $w = 2$ units and centred as follows:

- **Poor hypothesis** at $l_b + w/2$ where l_b is the lower bound of the search space.
- **Weak hypothesis** at $opt - 0.2 * (opt - l_b) - w/2$.
- **Good hypothesis** at opt .

We assess HypBO empirically in two different settings. First, we evaluate its performance and robustness against the quality of the hypothesis. Second, we test its ability, when faced with mixed hypotheses simultaneously, to discard the weaker hypotheses and prioritize promising ones.

Optimization with a single hypothesis Figure 2 shows that HypBO benefits from informative hypotheses and can also recover from weak ones. The method improves the search performance dramatically over the two baseline comparisons for a good hypothesis. The seeds from that hypothesis aid in recognizing the promising subspace and focusing efforts there, resulting in a faster location of the optimum. Many BO variants suffer from the boundary issue where BO typically spends many iterations at the boundary (Swersky 2017). This is particularly evident in the Ackley₄₉ task, where LA-MCTS stays in the boundaries for some time. In contrast, HypBO deals with that by exploring not only the

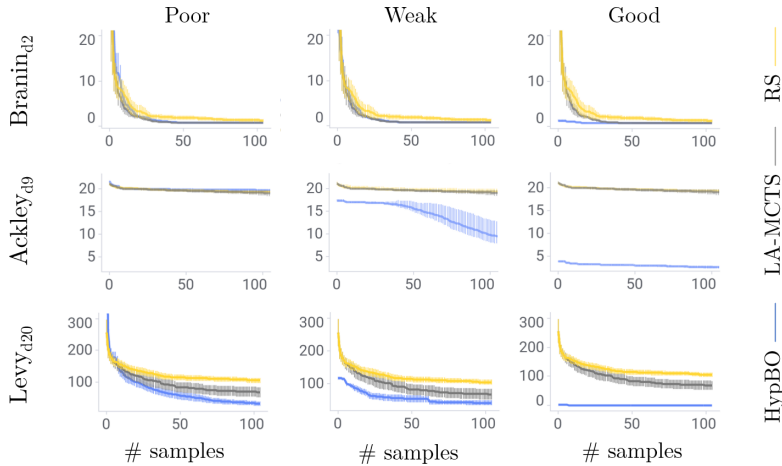


Figure 2: Comparison of HypBO, LA-MCTS and RS on Branin, Ackley, and Levy for various hypothesis qualities (see Fig. 1). Solid lines show the mean values, while the shaded areas represent the standard error.

Functions	LA-MCTS	RS	Good \mathcal{H}	Weak \mathcal{H}	Poor \mathcal{H}
Branin _{d2}	$0.80 \pm 1.42\text{E-}4$	1.31 ± 0.31	$0.80 \pm 7.05\text{E-}6$	$0.80 \pm 1.56\text{E-}4$	$0.80 \pm 3.91\text{E-}4$
Sphere _{d2}	$0.00 \pm 5.58\text{E-}5$	0.37 ± 0.18	$0.00 \pm 2.01\text{E-}7$	$0.00 \pm 7.01\text{E-}5$	$0.00 \pm 1.20\text{E-}4$
Ackley _{d5}	13.89 ± 3.00	16.80 ± 0.89	0.69 ± 0.41	7.67 ± 1.24	15.816 ± 2.76
Ackley _{d9}	19.05 ± 0.65	19.30 ± 0.35	2.64 ± 0.26	9.35 ± 1.62	19.71 ± 0.22
Rosenbrock _{d14}	5.77 ± 4.35	63.14 ± 9.42	$0.00 \pm 2.08\text{E-}3$	0.49 ± 0.22	0.91 ± 0.22
Levy _{d20}	69.01 ± 15.85	106.15 ± 7.84	0.18 ± 0.15	43.26 ± 7.08	32.76 ± 7.13

Table 1: Simple regret on synthetic functions with various dimensionalities. Best performance appears boldfaced.

hypothesis subspace but also its surroundings, which might be more promising, making it improve over the initial design. This behavior is emphasized with the weak hypothesis where these seeds, by outperforming the existing samples in the dataset, direct HypBO towards the hypothesis' surroundings, too, thus leading HypBO to converge toward the optimum faster than LA-MCTS. This highlights HypBO's ability to exploit the explicit and implicit information the hypothesis provides. As would be expected, poor hypotheses lead to a slower search in the early stages, but HypBO displays desired robustness by recovering from the poor seeds to approximately equal regret as LA-MCTS, as shown in Table 1. On this point, it is interesting to note that in the highest dimension case of Rosenbrock_{d14} and Levy_{d20}, the seeds from the poor hypothesis, being the worst samples in the search space, sensibly steer HypBO away from that area of the space, which in turn brings it closer to the optimal area. Signed-tests at a confidence level of 0.05 with a Bonferroni correction (Bonferroni 1936) show there is strong evidence (p-value of 0.55) for HypBO with good and weak hypotheses performing better than LA-MCTS and there is no difference (p-value of 1) between LA-MCTS and HypBO with poor hypothesis.

Optimization with mixed hypotheses Here, we use three different binary combinations of hypotheses of varying quality to test HypBO's ability to uncover and prioritize promising ideas, and to discard bad ideas from a pool of hy-

potheses. HypBO takes seeds from all the given hypotheses, which it uses to update its beliefs about each hypothesis via the MAB procedure. As the optimization progresses, it has a better representation of the hypotheses and can abandon the weaker one of the pair and select seeds from the more promising hypothesis. As shown in Figure 3, for the Ackley_{d9} function, this approach allows HypBO to deselect the weaker hypothesis early on. It keeps the remaining stronger hypothesis, which it uses to expedite the search, thereby considerably outperforming LA-MCTS and RS, as described in the previous subsection. Even in the case of combined weak and poor hypotheses, HypBO outperforms LA-MCTS and RS for the most part, or has equal regret performance, demonstrating its robustness when faced with multiple items of inaccurate knowledge and the ability to use these for better sampling. Table 2 shows that these findings are consistent when applied to a variety of other synthetic functions of higher dimensions. For lower dimensions, HypBO with mixed hypotheses has equal regret performance to LA-MCTS because the search space is smaller, and it becomes easier to capture the underlying behavior of the objective function. Here, the Bonferroni correction (Bonferroni 1936) shows there is strong evidence (p-values of 0.55) for HypBO with mixed hypotheses performing better than LA-MCTS.

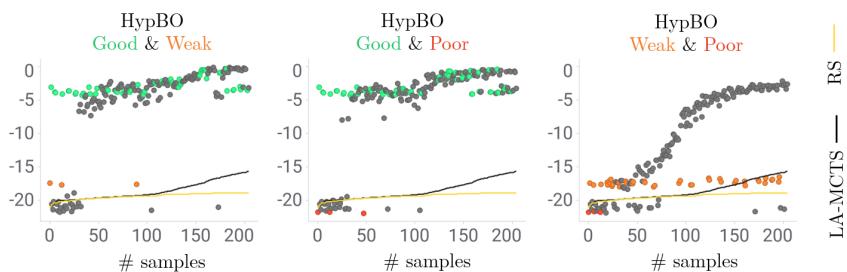


Figure 3: HypBO on the 9D-Ackley function with three different mixtures of hypotheses of various qualities for 200 iterations. Colored sample points came from the hypotheses, i.e. the lower level, while the grey ones come from the upper level. These different HypBO optimizations are compared against the mean of 50 trials of LA-MCTS and RS.

Functions	LA-MCTS	RS	Good & Poor \mathcal{H}	Good & Weak \mathcal{H}	Weak & Poor \mathcal{H}
Branin _{d2}	$0.80 \pm 1.42\text{E-}4$	1.31 ± 0.31	$0.80 \pm 7.41\text{E-}6$	$0.80 \pm 6.87\text{E-}6$	$0.80 \pm 1.436\text{E-}4$
Sphere _{d2}	$0.00 \pm 5.58\text{E-}5$	0.37 ± 0.18	$0.00 \pm 2.70\text{E-}7$	$0.00 \pm 3.26\text{E-}7$	$0.00 \pm 9.91\text{E-}5$
Ackley _{d5}	13.89 ± 3.00	16.80 ± 0.89	0.59 ± 0.36	0.90 ± 0.44	8.39 ± 1.32
Ackley _{d9}	19.05 ± 0.65	19.30 ± 0.35	2.72 ± 0.20	2.60 ± 0.25	10.45 ± 1.74
Rosenbrock _{d14}	5.77 ± 4.35	63.14 ± 9.42	$0.00 \pm 1.93\text{E-}3$	$0.01 \pm 2.99\text{E-}3$	0.44 ± 0.08
Levy _{d20}	69.01 ± 15.85	106.15 ± 7.84	0.24 ± 0.20	0.21 ± 0.18	15.01 ± 4.83

Table 2: Simple regret on synthetic functions with mixed hypotheses. Best performance appears boldfaced.

4.3 Photocatalytic Hydrogen Production Optimization

In this section, we test HypBO on a real materials design problem where we seek an optimal composition of ten materials to maximize hydrogen production through photocatalysis (Wang, Li, and Domen 2019). Due to the combinatorially large search space (98,423,325 possible combinations), Burger et al. 2020 used an autonomous mobile robotic chemist along with a discretized Bayesian optimizer (DBO), which can discretize the input space, to search for the optimal combination of materials.

We recast this experimental problem as a more cost-effective multivariable simulation; that is, we mapped out the chemical space by interpolating available experimental observations using a GPR. Specifically, this GPR model has a zero mean, a Matérn ($\nu = 2.5$) kernel with constant scaling and homoscedastic noise; each experimental variable length-scale λ_i is equal to its discretization step. We fitted this model against a total ‘ground truth’ dataset of 1119 experimental observations supplied by the authors of Burger et al. 2020. While the interpolated model is only approximate, close inspection suggested that it is broadly representative of the known real chemical space and sufficiently accurate to draw safe conclusions here. Our main motivation is to test whether we can capture and inject experts’ knowledge and intuition towards a better-informed and faster search. Here, to allow for a fair comparison, in place of LA-MCTS, we use the same DBO developed by Burger et al. for experimental photocatalysis hydrogen production as a baseline.

Retrospective Application of Knowledge First, we used HypBO to fold in, retrospectively, knowledge of the underlying chemistry that was not captured in the Burger et al. 2020 study to investigate whether injecting such hypothe-

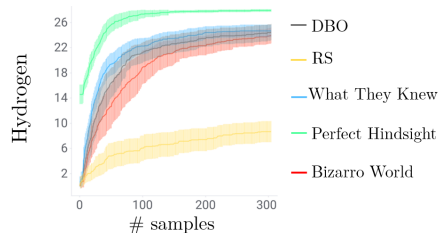


Figure 4: Retrospective application of hypotheses derived from Burger et al. 2020 using HyBO, compared to the no hypothesis run using DBO and RS. The shaded area represents the standard deviation.

ses might improve performance. We explored three separate cases, outlined briefly below with more detailed explanations in the Supplementary Material:

- **What They Knew** In 2019, there was extra chemical knowledge available prior to the Burger et al. 2020 study that could not have been injected using DBO; here, that knowledge is injected, retrospectively, using HypBO.
- **Perfect Hindsight** limits the search to within the optimal subspace based on *post facto* knowledge of the outcomes of all 1119 robotic experiments.
- **Bizarro World** purposefully focuses the search within the worst areas of the chemical space in all dimensions.

As shown in Figure 4, HypBO with ‘What They Knew’ boosts performance somewhat in the early stages of the search, and overall it improves upon DBO, thus validating the benefits of considering expert hypotheses in real-world problems. For example, one can posit that any or all of the

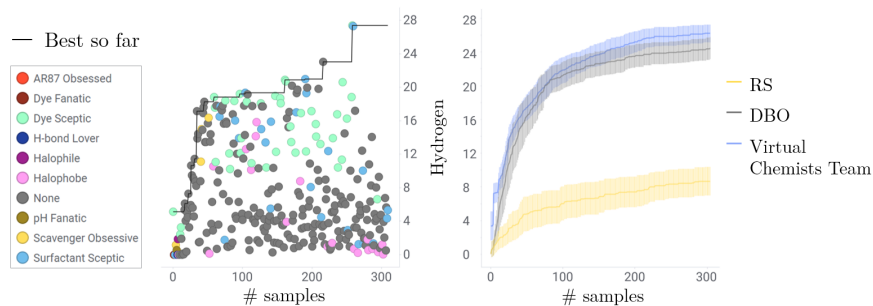


Figure 5: HypBO iteratively pruning the hypotheses and selecting seeds from the most promising ones to boost the optimization. Left: Scatter plot of the HypBO optimization iterations with all 9 virtual hypotheses; color of the points denotes the hypothesis followed, if any. Right: Best value obtained so far by HypBO with using all 9 hypotheses compared to DBO and RS.

three dye components (MB, AR87, RB) might be beneficial but that high values would be counterproductive, based on chemical reasoning. We captured this in 'What They Knew' by lowering the dyes' upper bounds ($MB \leq 0.5mL$, $AR87 \leq 1mL$, $RB \leq 0.5mL$). The somewhat modest boost given by 'What They Knew' (Figure 4) can be explained by the partial knowledge available in 2019; indeed, some of 'what they knew' was, in fact, wrong. For example, as reported in Burger et al. 2020, all three dyes were strongly negative at all concentrations. We have not captured this post-experiment knowledge here; rather, 'What They Knew' captures the knowledge that was available to this team in 2019, building on their initial formulation of hypotheses, prior to any robotic experiments.

Unsurprisingly, 'Perfect Hindsight' leads to a much faster optimization. By contrast, although the artificially bad case of 'Bizarro World' does lead to a slower search than DBO, the effects are greatly mitigated because HypBO can abandon unproductive hypotheses.

Searching the Chemistry Experiment Space with Mixed Hypotheses Here, we test HypBO's ability to exploit good hypotheses and discard bad ones in a more realistic setting by creating a team of nine 'virtual chemists', each with a virtual hypothesis based on plausible chemical reasoning that is detailed in the Supplementary Material. The combined 'knowledge' of this virtual team was then used to redo the GRS-simulated experiment for Burger et al. 2020 in tandem with HypBO. The virtual team was designed to emulate the diverse and sometimes contradictory views of a real research team tackling a new problem. For example, some pairs of hypotheses (e.g., 'Halophile' / 'Halophobe') are in direct contradiction. Based on retrospective knowledge, 'Dye Sceptic' and 'Surfactant Sceptic' might be expected empirically to be the strongest hypotheses, while 'Dye Fanatic' is probably the weakest. We applied all nine virtual hypotheses simultaneously and used the same oracle model described in the section above. For the purposes of these initial tests, all virtual hypotheses were considered to have equal weighting. Figure 5 illustrates the power of including human insights throughout the optimization. All nine hypotheses were selected initially, but as the optimization progressed, HypBO filtered out bad hypotheses and prioritised

the most promising ones, improving the search compared to DBO and RS. While the least profitable hypotheses, such as 'AR87 Obsessed', 'Dye Fanatic', and 'Halophobe', were deselected early on, HypBO does not discard them completely. For example, 'Halophobe' was selected at times when its EI was greater than others that were available for evaluation. This captures the importance of re-evaluating hypotheses in the face of new data. Likewise, certain hypotheses are used while they profitable and then discarded when they become delimiting; this can be observed for 'Scavenger Obsessive', where some scavenger is indeed required, but not too much. The modest search improvement of the virtual chemist team over DBO (Figure 5, right) is somewhat arbitrary because we purposefully built this virtual team to be mediocre, with both 'good' and 'bad' hypotheses in near equal number.

5 Conclusions

To fully exploit the opportunities presented by laboratory robotics and automation, we need multivariate optimization methods that work in partnership with teams of human scientists. So far, BO has not fully leveraged the experience and hunches of expert experimenters. We harness that knowledge here by allowing experimenters to inject their hypotheses about which parts of the input space will yield the best performance. We propose a BO variant, HypBO, that achieves this by recursively pruning and turning the hypotheses into seeds that augment sampling as a springboard for global optimization. HypBO's knowledge injection is more intuitive for users. It can also use weak hypotheses to converge faster than cases no hypotheses, and recover from poor ones. This highlights the power of human-computer interaction, re-imagining the role of humans in autonomous scientific discovery.

Future work will include further ablation studies. We also plan to initialize the human hypotheses with weights based on the experimenter's profile or confidence estimation. These weights will translate into HypBO's hypothesis beliefs and be updated throughout the optimization. This might be particularly valuable in quickstarting hypothesis selection in large, diverse research teams, where expertise levels and domain specializations can vary quite widely.

Appendix A Ten-dimensional Model for Hydrogen Production

In Section 4.3 of our work (Photocatalytic Hydrogen Production Optimization), we test HypBO against a real chemical problem. To do that, we constructed a ten-dimensional model describing hydrogen production for the experiments described in Burger et al. 2020. To do this, we augmented the original dataset of 688 experiments with a further 431 new experiments carried out under identical conditions and supplied by the authors of Burger et al. to create a total 'ground truth' dataset of 1119 experimental observations. The model was then built by fitting a Gaussian process regression (GPR) against the augmented dataset with a composite kernel consisting of Matern similarity, constant scaling and homoscedastic noise kernels. This hybrid kernel allows for variable smoothness and simulated experimental noise. Figure 6, below, shows the experimental data (blue and red points) plotted along with 812 "virtual" data points derived from this model (green points) in all ten dimensions. These plots suggest that the model adequately captures the behaviour described by the combined experimental dataset. It should be noted that the new experiments found compositions that produce more hydrogen than any compositions reported in Burger et al. 2020. We believe that this is reasonable because the dimensionality of the search space (10 variables) is large compared to the original experiment run (688 experiments), and there was no guarantee of optimality in that search. Notably, the GPR model reproduces the strongly negative influence of the three dyes, RB, AR87 and MB, (Figure 6a–c). It also appears that the new set of experiments (red points) might have discovered a new sub-space where NaCl contributes to the hydrogen production (Figure 6h).

Appendix B Retrospective Hypotheses about the Photocatalytic Hydrogen Production

This section refers to the "Retrospective Application of Knowledge" subsection and describes the mathematical representation of the retrospective hypotheses we derived from the work of Burger et al. to use with HypBO. In that study, they detailed, in their description of the design of the experiment, some additional chemical knowledge they had about photocatalytic hydrogen production that was not captured by their discretized Bayesian optimizer (DBO). The optimizer could not account for this knowledge, which here constitutes the retrospective knowledge that we refer to in the paper as "What they knew". Additionally, Burger et al.'s chemistry experiment made 688 experimental observations that lasted 8 days, extended here with a further 431 experiments supplied by the same team. By analyzing this augmented dataset of 1119 experiments, we derived two artificial items of knowledge. One is "Perfect Hindsight", which represents the subspace of best samples found to maximize hydrogen production, while the other is "Bizarro World", which represents the subspace of samples known to minimize hydrogen production.

B.1 What They Knew

To generate the hypothesis for the "What they knew" optimization test, a series of 10 sub-hypotheses was created based on mathematical constraints to capture the additional untapped chemistry knowledge of Burger et al., or at least what they thought they knew, prior to the experiments that were carried out in Burger et al. 2020. These ten constraints, and the associated chemical rationale, are listed below. The hypotheses were constructed from a combination of facts stated in the Burger et al. paper and more general chemical reasoning that would be available to any typical chemist. For example, Burger et al. set up their experiments so that the total volume was always 5 mL: as such, if 5 mL of any single component is added, then this does not leave any space for other components, and hence this might be too much.

Hypothesis 1. $P10 = 5\text{mg}$ Chemical rationale: Generally, the amount of hydrogen produced in photocatalytic systems increases with the amount of semiconductor photocatalyst (in this case, P10). Hence, in the total range of 1–5 mg that Burger et al. allowed, there was no obvious reason not to add the maximum amount of P10 since the hydrogen evolution rate—the search objective—was an absolute value that was not normalized to the mass of P10. This constraint ($P10 = 5\text{ mg}$) effectively removes one dimension from the search space.

Hypothesis 2. $Cys = 1 - 4\text{mL}$ Chemical rationale: Burger et al. stated that some cysteine would be required; that is, $Cys > 0$, because this is a sacrificial hydrogen production reaction, but it was not known, prior to experiments, how much cysteine would be optimal. However, because they constrained the maximum volume of the mixture of compounds to be 5 mL, then it might be undesirable to set, say, $Cys > 4\text{mL}$ since this would not then allow enough volume for adding other components. Using this simple reasoning, a range of $Cys = 1 - 4\text{mL}$ can be hypothesized, rather than the range of $Cys = 0 - 5\text{mL}$ that was used in the original experiments in Burger et al. 2020.

Hypothesis 3. $MB < 0.5\text{mL}$ Chemical rationale: Burger et al. expressed that adding dyes to the reaction was based on earlier observations that dyes could sensitize related photocatalysts, thus increasing hydrogen production (Wang et al. 2018). However, as mentioned in Burger et al. 2020, it was not known before experiments whether these three dyes (MB, AR87, RB) would be positive or negative in the case of P10. Still, one might reasonably expect that very high dye concentrations (e.g., $> 4\text{mL}$) could (a) absorb all of the light, thus lowering the hydrogen evolution rate, and (b) not leave enough volume for other components, as argued for Cys, above. Given the high light absorption coefficients of these three dyes, we conjecture that 'a little' might be enough; as such, a constraint of $MB < 0.5\text{mL}$ was formulated.

Hypothesis 4. $RB < 0.5\text{mL}$ Chemical rationale: Exactly as for MB (Hypothesis 3).

Hypothesis 5. $AR87 < 1\text{mL}$ Chemical rationale: As above for the dyes MB and AR87 except that here, the up-

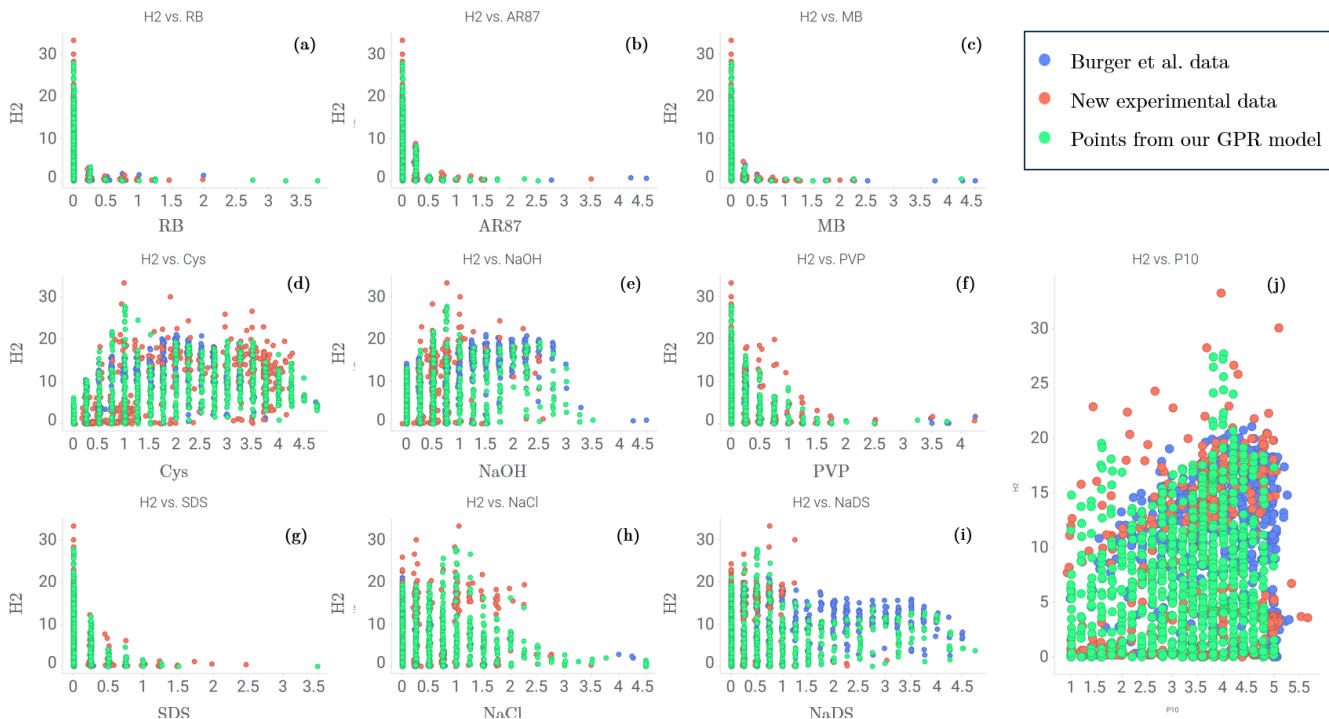


Figure 6: Plots showing the amount of hydrogen produced for 688 original experiments (blue points, (Burger et al. 2020)) and for 431 new experiments, supplied by the same authors, conducted under the same conditions (red points). The green points (812 data points shown here) are derived from a model fitted against a combination of these two experimental datasets.

per range, 1 mL, is larger because there was pre-existing evidence in (Wang et al. 2018) that this dye (called Eosin Y in that paper) could sensitize a related photocatalyst. As such, this dye might have been given a higher upper bound prior to experiments even though, in reality, Burger et al. found it to be a negative component in the reaction mixture.

Hypothesis 6. $NaOH < 3mL$ Chemical rationale: Burger et al.’s rationale for including NaOH was that solution pH might influence hydrogen production, but it was not known whether this would be positive or negative. A chemist might also have a potential concern that high concentrations of NaOH might degrade other components in the mixture, although this was not discussed by Burger et al. Also, as for Cys (Hypothesis 2), there is an argument for constraining the volume of NaOH to allow free volume for adding other components. These combined arguments led us to an estimated constraint of $NaOH < 3mL$, allowing (unlike Hypothesis 2) for a value of NaOH = 0 since from our reading of Burger et al. it was not obvious, *a priori* before experiment, that NaOH addition would have any positive effect.

Hypothesis 7. $NaCl < 3mL$ Chemical rationale: There was no *a priori* evidence that NaCl would be either positive or negative before experiments; as such, the constraint of 3 mL is to allow sufficient free volume for other components, exactly as for Hypothesis 6 above.

Hypothesis 8. $SDS < 1mL$ Chemical rationale: It was argued in (Burger et al. 2020) that the primary rationale

for adding surfactants was that it could aid in dispersing the photocatalysis, P10, in water. There was no evidence for this prior to the experiment. Still, given the highly surface-active nature of SDS, we might have hypothesized that a little surfactant could be enough, as argued for the three dyes (Hypotheses 3–5), hence $SDS < 1mL$.

Hypothesis 9. $PVP < 2mL$ Chemical rationale: PVP is also a surfactant, and hence the rationale is the same as for SDS (Hypothesis 7) – the larger range allowed here (maximum 2 mL instead of 1 mL) is because PVP is less surface-active than SDS at a given concentration. Hence, a higher volume might be required to be effective.

Hypothesis 10. $NaDS < 4mL$ Chemical rationale: As for NaOH (Hypothesis 6) – no prior information was available for the effect of this component, so the constraint arises from the need to allow some residual volume for other components, e.g., for CyS, which should be non-zero (see Hypothesis 2).

B.2 Perfect Hindsight

This hypothesis limits the search to within the optimal subspace based on *post facto* knowledge of the outcomes of all 1119 robotic experiments (see Figure 6). It is described by the following ten constraints:

1. $P10 \geq 3.5 mg$
2. $1 mL \leq Cys \leq 3.5 mL$
3. $0.5 mL \leq NaOH \leq 2 mL$

4. $0 \text{ mL} \leq \text{NaDS} \leq 1.5 \text{ mL}$
5. $2 \text{ mL} \leq \text{Cys} + \text{NaOH} + \text{NaDS} \leq 4.5 \text{ mL}$
6. $1 \text{ mL} \leq \text{NaCl} + \text{NaDS} + \text{NaOH} \leq 2.75 \text{ mL}$
7. $\text{MB} = 0 \text{ mL}$
8. $\text{AR87} = 0 \text{ mL}$
9. $\text{RB} = 0 \text{ mL}$
10. $\text{NaCl} < 2.5 \text{ mL}$
11. $\text{SDS} = 0 \text{ mL}$
12. $\text{PVP} = 0 \text{ mL}$

B.3 Bizarro World

This hypothesis limits the search to within the subspace of samples known to minimize the hydrogen production, based on *post facto* knowledge of the outcomes of all 1119 robotic experiments. It is described by the following ten constraints:

1. $\text{P10} = 1 \text{ mg}$
2. $\text{Cys} = 0 \text{ mL}$
3. $\text{MB} > 0.5 \text{ mL}$
4. $\text{AR87} > 0.5 \text{ mL}$
5. $\text{RB} > 0.5 \text{ mL}$
6. $\text{NaOH} = 0 \text{ mL}$
7. $\text{NaCl} > 0.5 \text{ mL}$
8. $\text{SDS} > 0.5 \text{ mL}$
9. $\text{PVP} > 0.5 \text{ mL}$
10. $\text{NaDS} = 0 \text{ mL}$

Appendix C Virtual Chemists

This section refers to the subsection ‘‘Searching the Chemistry Experiment Space with Mixed Hypotheses’’, in which we test HypBO’s ability to exploit good hypotheses and discard bad ones in a more realistic setting. This test mimics an experiment designed by a research team that holds a range of different opinions. To do this, we created nine ‘virtual chemists’ who hold hypotheses based on plausible chemical reasoning, which is outlined below. We purposefully designed this virtual team to be in conflict, with ‘good’ and ‘bad’ hypotheses in near equal numbers. As such, this is a deliberately mediocre virtual team: it was built to test the ability of HypBO to sort good and bad hypotheses, rather than to create a performance boost in the optimization, although as shown in the main text, it does in fact give a small improvement to the search.

C.1 Virtual Chemist #1: ‘‘Dye Sceptic’’

This chemist does not believe that dyes will have a positive effect on the reaction but has no other opinions about the value of other components in the mixture (that is, all other variables are allowed to range between the original low–high values when this hypothesis is applied). This hypothesis is expressed by the following constraints:

1. $\text{MB} = 0 \text{ mL}$
2. $\text{AR87} = 0 \text{ mL}$
3. $\text{RB} = 0 \text{ mL}$

C.2 Virtual Chemist #2: ‘‘Dye Fanatic’’

This chemist believes that dyes will have a positive effect and that a high dye concentration is required to achieve this; for example, to push the chemical equilibrium to achieve surface dye absorption on the photocatalyst. However, this chemist does not know which dye is best (all three are equally likely). Hence the *total* dye concentration is constrained to be greater than 3 mL; again, this chemist has no opinions about other components in the reaction. This hypothesis is expressed by the following constraints:

1. $\text{MB} + \text{AR87} + \text{RB} > 3 \text{ mL}$

C.3 Virtual Chemist #3: ‘‘AR87 Obsessed’’

Like Virtual Chemist #2, this chemist believes that dyes will have a positive effect but is convinced moreover that a specific dye, AR87, is optimal having read the earlier report that this dye was successful with other related photocatalysts (Wang et al. 2018). Virtual Chemist #3 believes that the other two dyes are likely to be less effective than AR87. As such, the recommendation of Virtual Chemist #3 is to ‘play in the dye space’ but with a strong emphasis on AR87, as expressed by:

1. $\text{AR87} > 3 \text{ mL}$
2. $\text{MB} < 0.5 \text{ mL}$
3. $\text{RB} < 0.5 \text{ mL}$

C.4 Virtual Chemist #4: ‘‘Surfactant Sceptic’’

This chemist believes that surfactants will be bad for the reaction but has no other opinions about any other components, as expressed by:

1. $\text{SDS} = 0 \text{ mL}$
2. $\text{PVP} = 0 \text{ mL}$

C.5 Virtual Chemist #5: ‘‘Scavenger Obsessive’’

This chemist is convinced that a very high concentration of the scavenger, Cys, is needed to achieve high levels of hydrogen production, as expressed by:

1. $\text{Cys} > 4 \text{ mL}$

C.6 Virtual Chemist #6: ‘‘pH Fanatic’’

This chemist believes high pH is needed to boost hydrogen production. Both NaOH and NaDS are bases and will increase the pH, and this chemist considers both to be interchangeable, leading to the hypothesis:

1. $\text{NaOH} + \text{NaDS} > 3.5 \text{ mL}$

C.7 Virtual Chemist #7: ‘‘H-bond Lover’’

This chemist believes that H-bonding with NaDS will lead to increased hydrogen production, based on reading earlier publications made similar hypotheses about NaDS, e.g., (Zhang et al. 2019), leading to the hypothesis:

1. $\text{NaDS} > 3.5 \text{ mL}$

C.8 Virtual Chemist #8: “Halophile”

This chemist believes that high ionic strength is crucial for the success of the reaction—that is, a high concentration of salt; NaOH, NaDS and NaCl are all salts, leading to the hypothesis:



C.9 Virtual Chemist #9: “Halophobe”

In contrast to Virtual Chemist #8, this chemist believes that high NaCl concentration is bad for the reaction because they half-remember seeing a conference presentation that claimed that NaCl addition can lead to chlorine gas production, rather than hydrogen production. This leads to the hypothesis:



Acknowledgements

The authors acknowledge financial support from the Leverhulme Trust via the Leverhulme Research Centre for Functional Materials Design. AIC thanks the Royal Society for a Research Professorship (RSRP\S2\232003).

References

- A V, A. K.; Rana, S.; Shilton, A.; and Venkatesh, S. 2022. Human-AI collaborative Bayesian optimisation. In Koyejo, S.; Mohamed, S.; Agarwal, A.; Belgrave, D.; Cho, K.; and Oh, A., eds., *Advances in Neural Information Processing Systems*, volume 35, 16233–16245. Curran Associates, Inc.
- Bonferroni, C. 1936. *Teoria statistica delle classi e calcolo delle probabilità*. Pubblicazioni del R. Istituto superiore di scienze economiche e commerciali di Firenze. Seeber.
- Burger, B.; Maffettone, P. M.; Gusev, V. V.; Aitchison, C. M.; Bai, Y.; yan Wang, X.; Li, X.; Alston, B. M.; Li, B.; Clowes, R.; Rankin, N.; Harris, B.; Sprick, R. S.; and Cooper, A. I. 2020. A mobile robotic chemist. *Nature*, 583: 237–241.
- Diouane, Y.; Picheny, V.; Riche, R. L.; and Perrotolo, A. S. D. 2021. TREGO: a trust-region framework for efficient global optimization. *Journal of Global Optimization*, 86: 1–23.
- Ebden, M. 2015. Gaussian processes: a quick introduction. arXiv:1505.02965.
- Eriksson, D.; Pearce, M.; Gardner, J.; Turner, R. D.; and Poloczek, M. 2019. Scalable global optimization via local Bayesian optimization. In Wallach, H.; Larochelle, H.; Beygelzimer, A.; d'Alché-Buc, F.; Fox, E.; and Garnett, R., eds., *Advances in Neural Information Processing Systems*, volume 32. Curran Associates, Inc.
- Hernández-Lobato, J. M.; Gelbart, M.; Hoffman, M.; Adams, R.; and Ghahramani, Z. 2015. Predictive entropy search for Bayesian optimization with unknown constraints. In *International Conference on Machine Learning*, 1699–1707. PMLR.
- Hickman, R. J.; Ruža, J.; Tribukait, H.; Roch, L. M.; and García-Durán, A. 2023. Equipping data-driven experiment planning for self-driving laboratories with semantic memory: case studies of transfer learning in chemical reaction optimization. *Reaction Chemistry & Engineering*.
- Huang, D.; Filstroff, L.; Mikkola, P.; Zheng, R.; and Kaski, S. 2022. Bayesian optimization augmented with actively elicited expert knowledge. arXiv:2208.08742.
- Hvarfner, C.; Stoll, D.; Souza, A.; Nardi, L.; Lindauer, M.; and Hutter, F. 2022. π BO: Augmenting acquisition functions with user beliefs for Bayesian optimization. In *10th International Conference on Learning Representations, ICLR'22*, 1–30.
- Häse, F.; Aldeghi, M.; Hickman, R. J.; Roch, L. M.; and Aspuru-Guzik, A. 2021. Gryffin: An algorithm for Bayesian optimization of categorical variables informed by expert knowledge. *Applied Physics Reviews*, 8(3): 031406.
- Jones, D. R.; Schonlau, M.; and Welch, W. J. 1998. Efficient global optimization of expensive black-box functions. *Journal of Global Optimization*, 13(4): 455–492.
- Köppe, M.; Queyranne, M.; and Ryan, C. T. 2010. Parametric integer programming algorithm for bilevel mixed integer programs. *Journal of Optimization Theory and Applications*, 146(1): 137–150.
- Li, C.; Gupta, S.; Rana, S.; Nguyen, V.; Robles-Kelly, A.; and Venkatesh, S. 2020. Incorporating expert prior knowledge into experimental design via posterior sampling. arXiv:2002.11256.
- Morishita, T.; and Kaneko, H. 2023. Initial sample selection in Bayesian optimization for combinatorial optimization of chemical compounds. *ACS Omega*, 8(2): 2001–2009.
- Niu, S.; Liu, Y.; Wang, J.; and Song, H. 2020. A decade survey of transfer learning (2010–2020). *IEEE Transactions on Artificial Intelligence*, 1(2): 151–166.
- Ramachandran, A.; Gupta, S.; Rana, S.; Li, C.; and Venkatesh, S. 2020. Incorporating expert prior in Bayesian optimization via space warping. *Knowledge-Based Systems*, 195: 105663.
- Shahriari, B.; Swersky, K.; Wang, Z.; Adams, R.; and De Freitas, N. 2016. Taking the human out of the loop: a review of Bayesian optimization. In *Proceedings of the IEEE*, volume 104, 148–175. Institute of Electrical and Electronics Engineers Inc. Publisher Copyright: © 1963-2012 IEEE.
- Siemenn, A. E.; Ren, Z.; Li, Q.; and Buonassisi, T. 2023. Fast Bayesian optimization of needle-in-a-Haystack problems using zooming memory-based initialization (ZoMBI). *npj Computational Mathematics*, 9: 79.
- Souza, A.; Nardi, L.; Oliveira, L. B.; Olukotun, K.; Lindauer, M.; and Hutter, F. 2021. Bayesian Optimization with a prior for the optimum. In Oliver, N.; Pérez-Cruz, F.; Kramer, S.; Read, J.; and Lozano, J. A., eds., *Machine Learning and Knowledge Discovery in Databases. Research Track*, 265–296. Cham: Springer International Publishing. ISBN 978-3-030-86523-8.
- Swersky, K. 2017. *Improving Bayesian optimization for machine learning using expert priors*. Ph.D. thesis, University of Toronto.

Theckel Joy, T.; Rana, S.; Gupta, S.; and Venkatesh, S. 2019. A flexible transfer learning framework for Bayesian optimization with convergence guarantee. *Expert Systems with Applications*, 115: 656–672.

Vermorel, J.; and Mohri, M. 2005. Multi-armed bandit algorithms and empirical evaluation. In Gama, J.; Camacho, R.; Brazdil, P. B.; Jorge, A. M.; and Torgo, L., eds., *Machine Learning: ECML 2005*, 437–448. Berlin, Heidelberg: Springer Berlin Heidelberg. ISBN 978-3-540-31692-3.

Wang, L.; Fonseca, R.; and Tian, Y. 2020. Learning search space partition for black-box optimization using Monte Carlo tree search. In Larochelle, H.; Ranzato, M.; Hadsell, R.; Balcan, M.; and Lin, H., eds., *Advances in Neural Information Processing Systems*, volume 33, 19511–19522. Curran Associates, Inc.

Wang, X.; Chen, L.; Chong, S. Y.-L.; Little, M. A.; Wu, Y.; Zhu, W.; Clowes, R.; Yan, Y.; Zwijnenburg, M. A.; Sprick, R. S.; and Cooper, A. I. 2018. Sulfone-containing covalent organic frameworks for photocatalytic hydrogen evolution from water. *Nature Chemistry*, 10: 1180–1189.

Wang, Z.; Li, C.; and Domen, K. 2019. Recent developments in heterogeneous photocatalysts for solar-driven overall water splitting. *Chem. Soc. Rev.*, 48: 2109–2125.

Zhang, J.; Li, J.; Su, H.; Zhao, Y.; Zeng, X.; Hu, M.; Xiao, W.; and Mao, X. 2019. H-bonding effect of oxyanions enhanced photocatalytic degradation of sulfonamides by g-C₃N₄ in aqueous solution. *Journal of Hazardous Materials*, 366: 259–267.